Electronic Supplementary Material (ESI) for Soft Matter

Pickering Emulsions Stabilized by Amphiphilic Nano-Sheets

Andres F. Mejia,[ab] Agustin Diaz,[c] Srinivasa Pullela,[a] Ya-Wen Chang,[a] Michael Simonetty,[a] Carrie Carpenter,[c] James D. Batteas,[cd] M. Sam Mannan,[abd] Abraham Clearfield,[c] and Zhengdong Cheng[abde]*

[a] Artie McFerrin Department of Chemical Engineering, Texas A&M University, College Station, TX, 77843-3122, USA. Email: zcheng@tamu.edu

[b] Mary Kay O'Connor Process Safety Center, Artie McFerrin Department of Chemical Engineering, Texas A&M University, College Station, TX, 77843-3122, USA

[c] Department of Chemistry, Texas A&M University, College Station, TX, 77843-3125, USA

[d] Materials Science and Engineering, Texas A&M University, College Station, TX, 77843-3003, USA

[e] Professional Program in Biotechnology, Texas A&M University, College Station, TX, 77843-3122, USA

Supporting Information

1. Particle-stabilized emulsions

Adsorption of homogeneous and amphiphilic particles at liquid-liquid interfaces

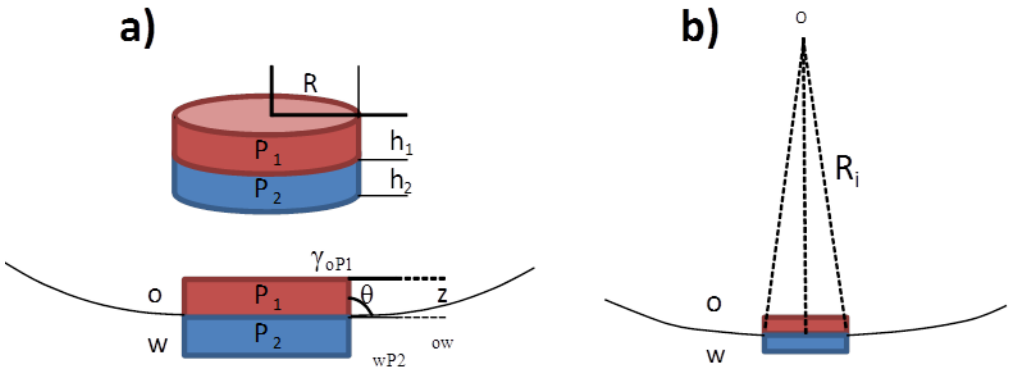

Fig. S1. Illustrations of **(a)** a disk-shaped Janus particle and **(b)** its interfacial adsorption. Modified according to Nonomura et al.[1]

Using homogeneous spheres, the highest stability of the resulting Pickering emulsion occurs when the three-phase contact angle among the particle, hydrophobic, and hydrophilic fluids is around 90°.[2-7] Hydrophobic particles will stabilize water-in-oil emulsions having a contact angle slightly greater than 90°, whereas hydrophilic particles will

stabilize oil-in-water emulsions having a contact angle slightly less than 90°.[2] In the case of Janus spheres, the stability is measured using the energy required to remove a particle from equilibrium into the hydrophobic fluid and normalized by the energy of removing it from the hydrophilic fluid, which is the so called Janus balance *J*, $J = (\sin^2\alpha+2\cos\theta_p(\cos\alpha-1))/(\sin^2\alpha+2\cos\theta_a(\cos\alpha+1))$, where α is the angle from the center of the sphere to the hydrophilic-hydrophobic boundary, θ_p is the contact angle of the hydrophilic side, and θ_a is the contact angle of the hydrophobic side. The highest stability of the Pickering emulsion stabilized by Janus particles is achieved when $J=1$, which can be obtained via tuning the parameter α.[8-10]

The energy necessary to remove a disk-shaped Janus particle from its equilibrium position at the oil-water interface along the boundary between the hydrophobic and hydrophilic hemispheres is defined by[1] $\Delta G_{min}=\pi R_d^2(\gamma_{oP1}+\gamma_{wP2}-\gamma_{ow})+2\pi R_d(h_1\gamma_{oP1}+h_2\gamma_{wP2})$, where πR_d^2 is the cross-sectional area of the particle, h_1 and h_2 are thickness of the hydrophobic and the hydrophilic regions, respectively, and the sum of them is equal to the thickness of the disk. P_1 indicates the hydrophobic region and P_2, the hydrophilic region. γ_{oP1} and γ_{wP2} are the interfacial energies between the hydrophobic or hydrophilic regions and the oil or water interfaces, respectively (**Fig. S1**). A similar behavior is presented for spherical[11] Janus particles.

Possible mechanism of emulsion stabilization by large aspect ratio nano-sheets.

However, two *opposite* effects are at work in the stabilization of Pickering emulsions using spherical particles, which have only one length scale, the diameter of the spheres $2r_s$. First, the interfaces of two adjacent emulsions will endure a maximum capillary pressure[12] right before coalescence (P_c^{max}), which can be expressed as $P_c^{max} = \pm p(2\gamma_{ow}/r_s)(\cos\theta \pm z)$, where p is a theoretical parameter used to link the influence of particle concentration (with a "+" sign referring to oil-in-water (o/w) emulsions and with a "–" sign referring to water-in-oil (w/o) emulsions), and z is a constant dependent upon on the arrangement of particles in the interface.[12] γ_{ow} is the interfacial energy between the oil and the water, θ is the three-phase contact angle at the interface and r_s is the radius of the spheres.[12-14] Assuming that θ is inside the stability intervals[12] and the inter-particle distance is fixed,[15] hence, the smaller the size of the spheres, the larger P_c^{max} can be.[12, 15] Spheres with a smaller radius r_s, therefore, prevent emulsion coalescence better than do larger spheres. Secondly, in the opposite effect, it is well known that small particles tend to escape from the interface by thermal fluctuations. The free energy to remove a sphere from the interface is defined by $\Delta G_{remove} = \pi r_s^2 \gamma_{ow}(1+\cos\theta)^2$. Therefore, spheres with a smaller radius r_s escape more easily from the interface by thermal fluctuation than do the larger spheres.

The highly *anisotropic* particles we used here could reconcile these two effects due to the existence of *two* length scales, thickness h and lateral size $2R_d$. When considering the capillary interaction between two nano-sheets, an amphiphilic nano-sheet in the interface is equivalent to a closed packing of spheres with the interstitial space filled, where $2r_s$ (diameter of each sphere) corresponds to the thickness of the nano-sheet h. Also, the total area covered by these spheres is equal to the area covered by the nano-sheet. The interfaces of two adjacent emulsions will endure a maximum capillary pressure as $P_c^{max} \approx \pm p(2\gamma_{ow}/r_s)(\cos\theta \pm z) \approx \pm p(4\gamma_{ow}/h)(\cos\theta \pm z)$. The nano-sheet thickness h can serve as a proxy for sphere diameter in the role of preventing emulsion coalescence. The capillary interaction between two nano-sheets with thickness h, with two edges parallel to each other, the meniscus between them is similar to that between two parallel cylinders of length h. The extremely small value of h offers a good capability to stabilize emulsions. Simultaneously, the nano-sheets' large lateral size $2R_d$ offers strong adsorption towards the interface, preventing its escape due to thermal motion. Thus, particles with a large cross-sectional area, πR_d^2, can be strongly adsorbed to the interface. Since $\Delta G_{remove} \sim R_d^2$ and $P_c^{max} \sim 1/h$, anisotropic particles with high aspect ratio ($\xi = 2R_d/h$) can be good emulsion stabilizers.[16] However, large nano-sheets in diameter result in larger interstitial spaces compared with smaller nano-sheets. But, the emulsion droplets are stable because the nano-sheets are drawn into the region of inter-droplet forming a dense bridging monolayer as a result of strong capillary attraction.[17, 18]

As Pickering stabilizers, high aspect ratio nano-sheets are more efficient than spheres. A nano-sheet has lower volume compared to a sphere of the same radius, hence less weight if the density is the same. For the same volume, a nano-sheet has a larger cross section on the interface, and adsorb stronger to the interface than a sphere. Therefore, fewer nano-sheets are required to cover the same liquid-liquid interface compared to their spherical counterparts.[19] In addition, a nano-sheet presents a lower diffusivity of molecules compared to a close-packed structure of spheres of the same area; hence, blocking the process of Ostwald ripening that result in a lower degree of coalescence.[15]

2. Synthesis and characterization of Zirconium Phosphate (ZrP)

Visualization of ZrP nano-sheets

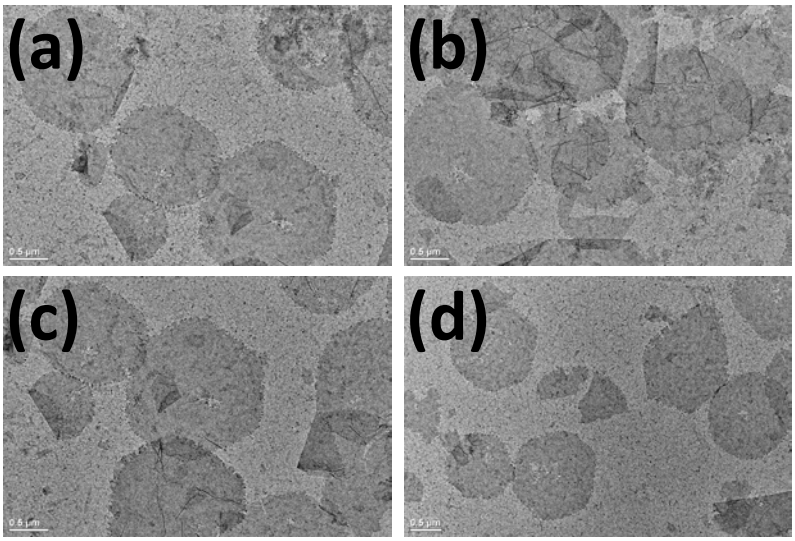

Fig. S2. Transmission electron microscope (TEM) micrographs of several non-modified α-ZrP nano-sheets.

The α-ZrP nano-sheets in **Fig. S2** are thin and flexible, and can present wrinkles as shown in **Fig. S2(b,c).** This demonstrates that the nano-sheets can bend on the oil-water interface to stabilize the emulsions. It has been proven that the single nano-plate layer is rigid when the nano-sheet size is about several tenths of a nanometer or less and becomes flexible when the size is larger than a hundred nanometers, depending on the bending elasticity of the layer.[20]

Control of the size of ZrP crystals via hydrothermal method

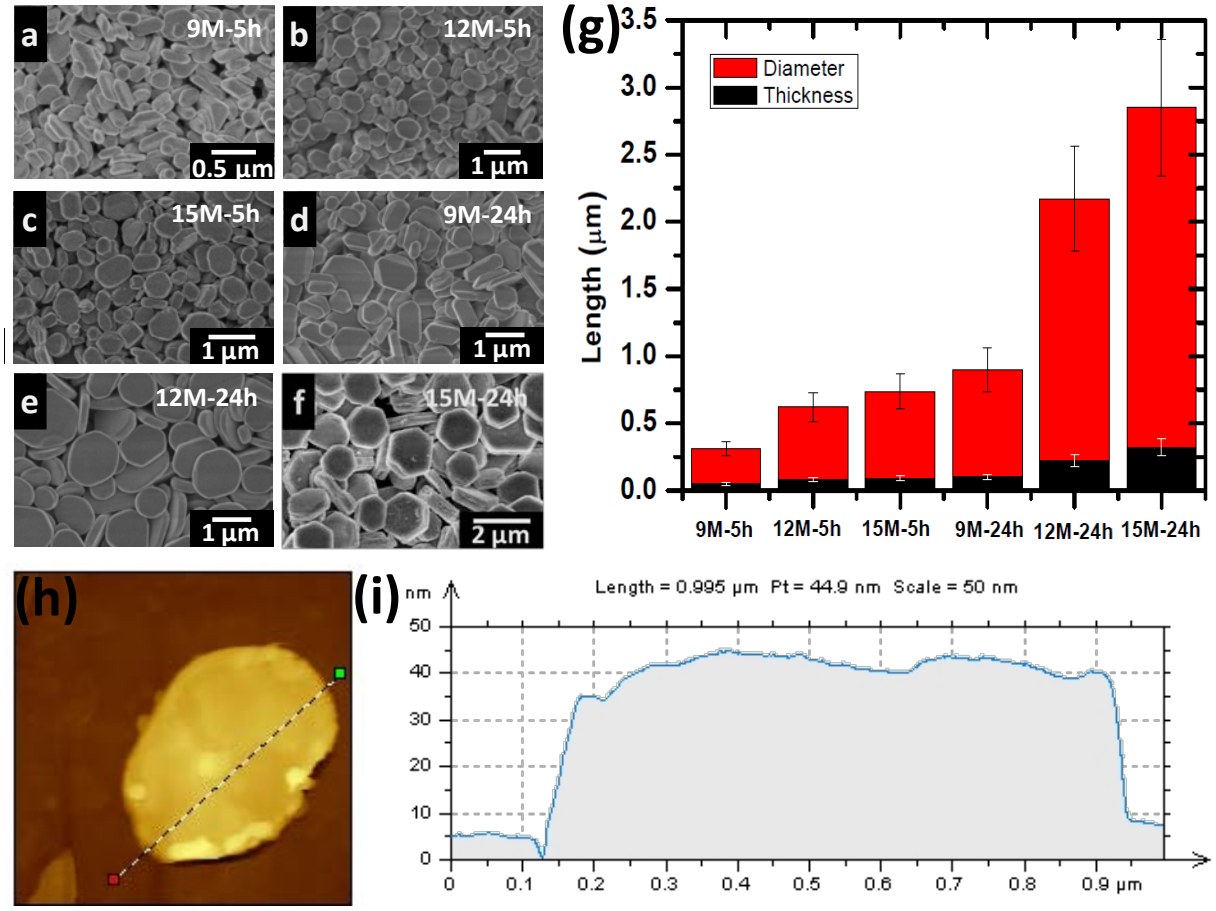

Fig. S3. Pristine α-zirconium phosphate crystals. Scanning electron microscope (SEM) micrographs of different α-ZrP sizes synthesized via the hydrothermal method at 200 ºC under different conditions (phosphoric acid concentration – reaction time). **(a)** 9M-5h, **(b)** 12M-5h, **(c)** 15M-5h, **(d)** 9M-24h, **(e)** 12M-24h, and **(f)** 15M-24h. **(g)** Quantification of the diameter (red bar) and the thickness (black bar) of the α-ZrP crystals.[21] **(h)** Atomic force microscope (AFM) contact mode topography image of a pristine α-ZrP crystal fabricated using 9M phosphoric acid for 24 h over a Si(100) surface modified with 3-aminopropyl trichlorosilane (APTES). **(i)** Section analysis for the cross-section white line seen in (h) gives a thickness of around 38 nm.

Characterization of the thickness of ZrP crystals via Atomic force microscopy (AFM)

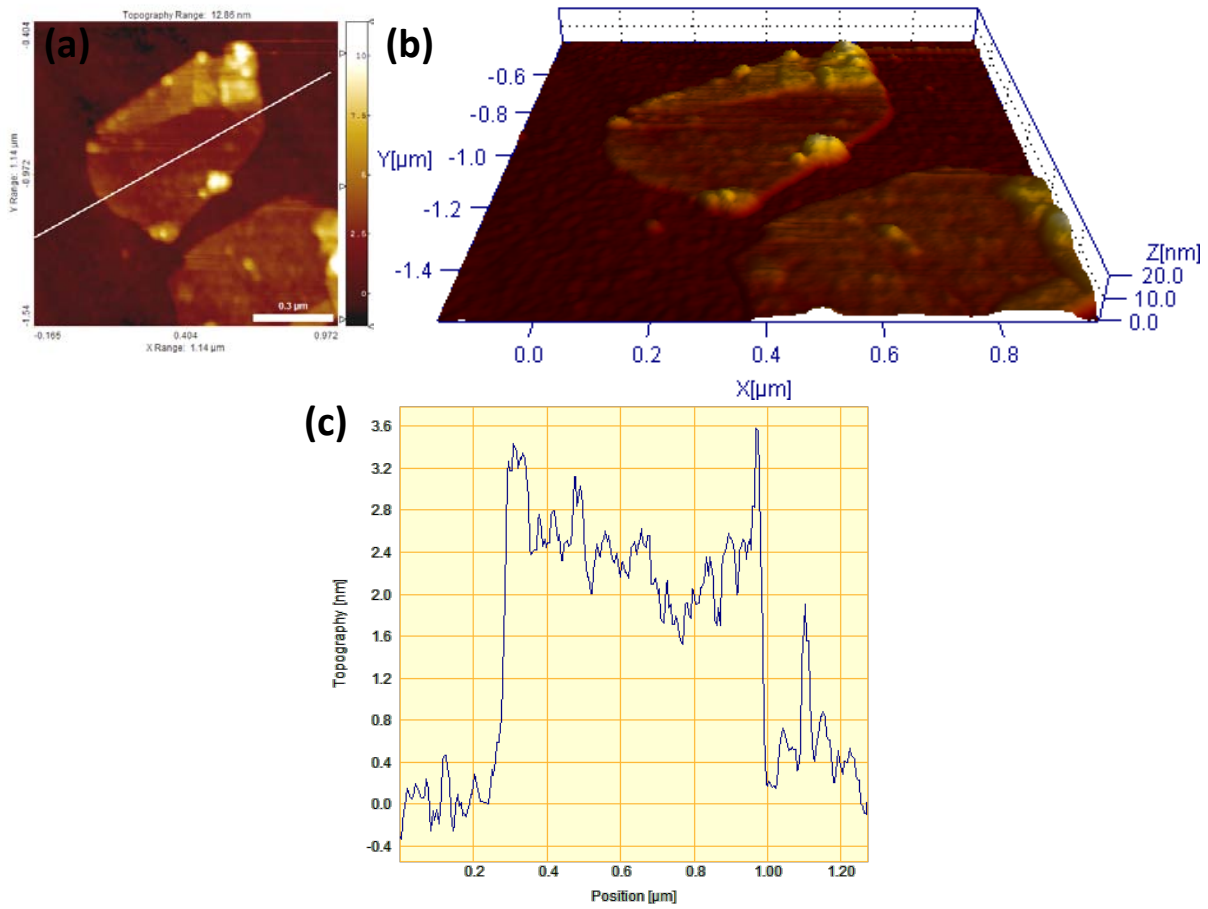

Fig. S4. Modified α-ZrP-ODI nano-sheet. AFM contact mode topography image and section analysis of an amphiphilic α-ZrP-ODI nano-sheet over a Si(100) surface modified with octadecyltrichlorosilane (OTS). **(a)** 2D, and **(b)** 3D topography images. **(c)** Section analysis gives a thickness of around 2.8 nm (0.63 nm of a α-ZrP monolayer and 2.17 nm of the aliphatic chain) for the cross-section white line seen in (a).

Monolayer films of the desired alkylsilanes (APTES or OTS) were first prepared on cleaned and oxidized Si(100) and then ZrP nano-plates (or nano-sheets) were deposited through self-assembly using a suspension of the ZrP nano-sheets (nano-sheets) in a suitable solvent (EtOH for APTES and toluene for OTS). Si(100) substrates were cleaned and hydroxylated with a basic piranha solution (4:1:1) (v:v:v) mixture of high purity H_2O: H_2O_2(30%):NH_4OH) at 80°C for 30 min. The substrates were rinsed under high-purity water for 60 s, then with ethanol, and finally dried under streaming nitrogen. Then the substrate was incubated in 1 wt % solutions of desired alkylsilanes (APTES or OTS) in a suitable solvent (EtOH for APTES and toluene for OTS) for ca. 15 h. The modified substrates were rinsed under high-purity water for 60 s, then with ethanol, and finally dried under streaming nitrogen. Finally, the ZrP nano-plates (or nano-sheets) were deposited through self-assembly using a suspension of the ZrP nano-sheets in a suitable solvent (EtOH for APTES and toluene for OTS) for 5 h. The final obtained substrate were rinsed under high-purity water for 60 s, then EtOH, and finally dried under streaming nitrogen.

3. Surface characterization of polystyrene particles stabilized by ZrP-ODI nano-sheets

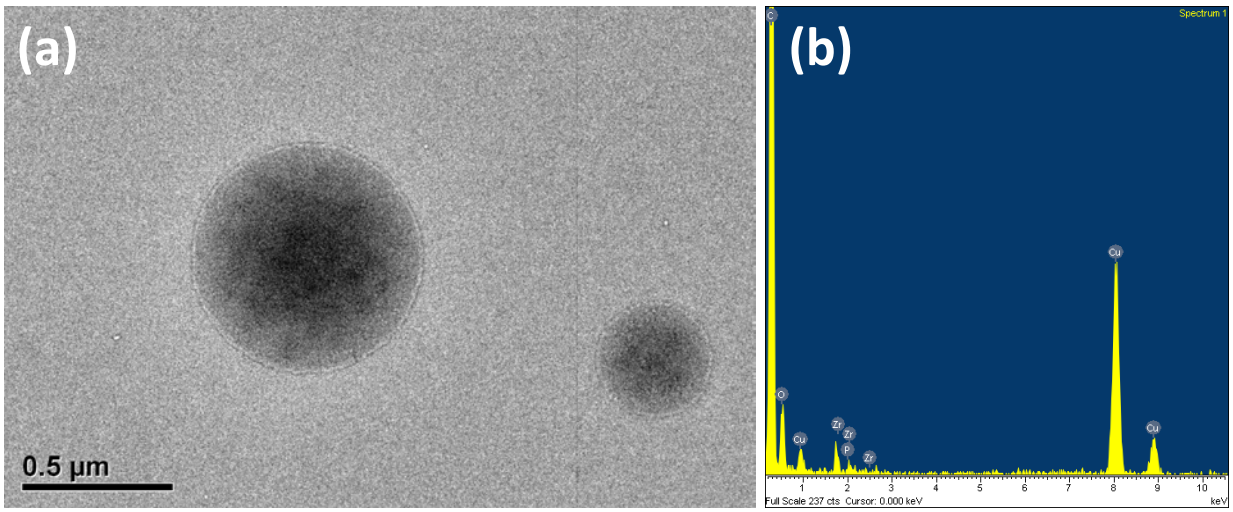

Fig. S5. TEM and EDX elemental mapping analysis of the polystyrene-α-ZrP-ODI-nano-sheet particles. **(a)** TEM micrograph **(b)** Surface EDX spectra.

4. Static contact angle measurements

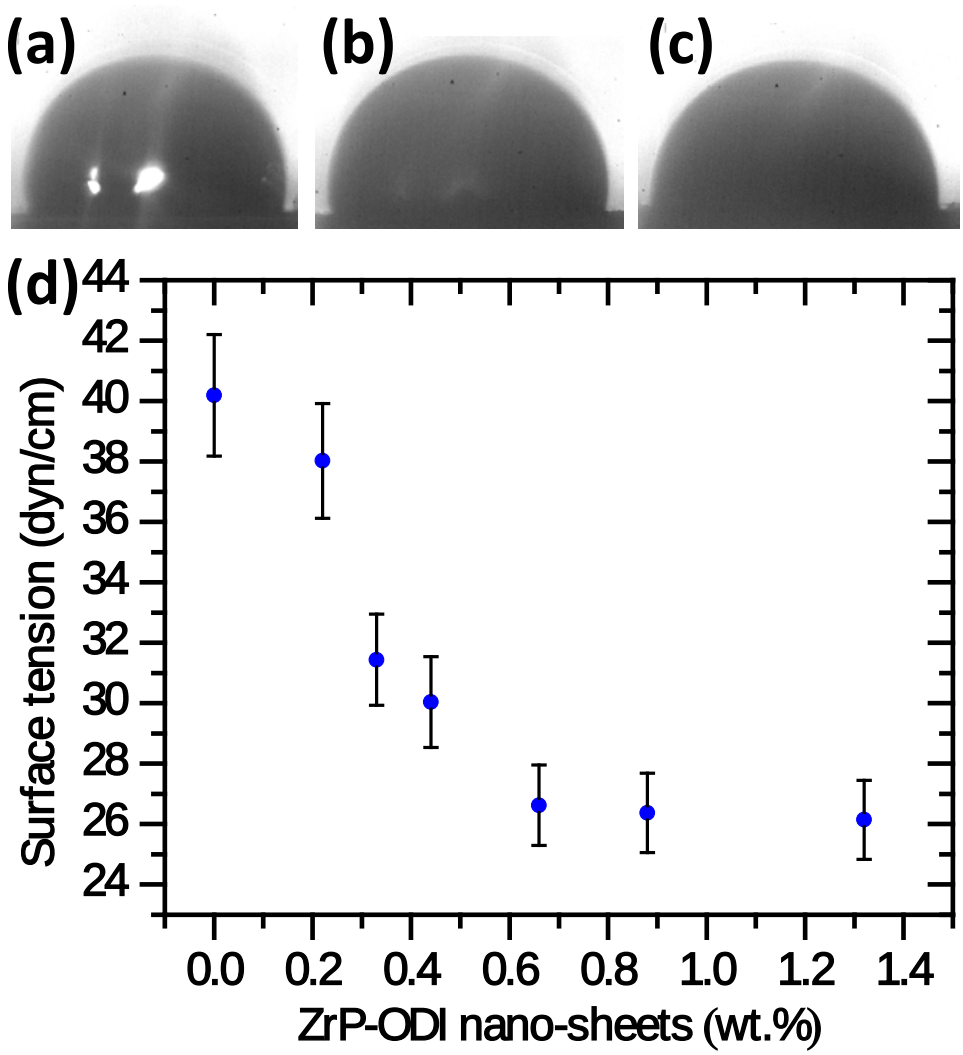

Fig. S6. Suspension droplets at different α-ZrP-ODI nano-sheet concentrations. **(a)** Water only, **(b)** 0.44 wt% α-ZrP-ODI nano-sheets, and **(c)** 1.32 wt% α-ZrP-ODI nano-sheets. **(d)** Plot of the PDMS/suspensions interfacial tension against α-ZrP-ODI nano-sheet concentration.

A Phantom V4.2 camera (Vision Research, Wayne, NJ) with a high-magnification lens, together with the active contours method for measuring high-accuracy contact angles using ImageJ[22] was used to measure the surface tension of the PDMS-water interface. A glass slide was coated with PDMS to simulate similar surface tension interactions as in a PDMS-in-water suspension. The static contact angles were measured for seven different samples at different α-ZrP-ODI nano-sheet concentrations, as shown in **Fig. S6**. Using Young's equation, $\gamma_{sl} = \gamma_{sa} - \gamma_{la}\cos\theta$, where γ_{sl}, γ_{sa} and γ_{la} correspond to the PDMS-liquid, PDMS-air and liquid-air surface tensions, respectively. The values taken for γ_{sa} was 21.8 dyn/cm[23] and for γ_{la} was 72.8 dyn/cm[24]. **Fig. S6** shows a similar tendency when compared to **Fig. 5a** and **Fig. 7**, where α-ZrP-ODI nano-sheet concentration between 0.2 to 0.62 wt. % caused a decrease in surface tension and polystyrene particle diameter.

References

1. Y. Nonomura, S. Komura and K. Tsujii, *Langmuir*, 2004, **20**, 11821-11823.
2. S. Melle, M. Lask and G. G. Fuller, *Langmuir*, 2005, **21**, 2158-2162.
3. B. P. Binks, *Curr. Opin. Colloid. In.*, 2002, **7**, 21-41.
4. N. P. Pardhy and B. M. Budhlall, *Langmuir*, 2010, **26**, 13130-13141.
5. S. Berger, A. Synytska, L. Ionov, K. J. Eichhorn and M. Stamm, *Macromolecules*, 2008, **41**, 9669-9676.
6. A. Perro, S. Reculusa, S. Ravaine, E. B. Bourgeat-Lami and E. Duguet, *J. Mater. Chem.*, 2005, **15**, 3745-3760.
7. X. Y. Ling, I. Y. Phang, C. Acikgoz, M. D. Yilmaz, M. A. Hempenius, G. J. Vancso and J. Huskens, *Angew. Chem.-Int. Edit.*, 2009, **48**, 7677-7682.
8. S. Jiang and S. Granick, *J. Chem. Phys.*, 2007, **127**.
9. E. M. Herzig, K. A. White, A. B. Schofield, W. C. K. Poon and P. S. Clegg, *Nat. Mater.*, 2007, **6**, 966-971.
10. B. P. Binks and P. D. I. Fletcher, *Langmuir*, 2001, **17**, 4708-4710.
11. C. Casagrande, P. Fabre, E. Raphael and M. Veyssie, *Europhys. Lett.*, 1989, **9**, 251-255.
12. G. Kaptay, *Colloid. Surface. A.*, 2006, **282-283**, 387-401.
13. N. D. Denkov, I. B. Ivanov, P. A. Kralchevsky and D. T. Wasan, *J. Colloid Interface Sci.*, 1992, **150**, 589-593.
14. T. N. Hunter, R. J. Pugh, G. V. Franks and G. J. Jameson, *Adv. Colloid Interface Sci.*, 2008, **137**, 57-81.
15. S. Tcholakova, N. D. Denkov and A. Lips, *PCCP*, 2008, **10**, 1608-1627.
16. B. Madivala, S. Vandebril, J. Fransaer and J. Vermant, *Soft Matter*, 2009, **5**, 1717-1727.
17. T. S. Horozov and B. P. Binks, *Angew. Chem.-Int. Edit.*, 2006, **45**, 773-776.
18. C. Zeng, H. Bissig and A. D. Dinsmore, *Solid State Commun.*, 2006, **139**, 547-556.
19. F. X. Liang, K. Shen, X. Z. Qu, C. L. Zhang, Q. A. Wang, J. L. Li, J. G. Liu and Z. Z. Yang, *Angew. Chem.-Int. Edit.*, 2011, **50**, 2379-2382.
20. W. J. Boo, L. Sun, G. L. Warren, E. Moghbelli, H. Pham, A. Clearfield and H. J. Sue, *Polymer*, 2007, **48**, 1075-1082.
21. L. Y. Sun, W. J. Boo, H. J. Sue and A. Clearfield, *New J. Chem.*, 2007, **31**, 39-43.
22. A. F. Stalder, G. Kulik, D. Sage, L. Barbieri and P. Hoffmann, *Colloid. Surface. A.*, 2006, **286**, 92-103.
23. M. K. Chaudhury and G. M. Whitesides, *Langmuir*, 1991, **7**, 1013-1025.
24. G. Vazquez, E. Alvarez and J. M. Navaza, *J. Chem. Eng. Data*, 1995, **40**, 611-614.